eNeuro

Research Article: New Research | Cognition and Behavior

Doublecortin-like is implicated in adult hippocampal neurogenesis and in motivational aspects to escape from an aversive environment in male mice

https://doi.org/10.1523/ENEURO.0324-19.2020

Cite as: eNeuro 2020; 10.1523/ENEURO.0324-19.2020

Received: 14 August 2019
Revised: 12 August 2020
Accepted: 14 August 2020

1. **Manuscript Title**
Doublecortin-like is implicated in adult hippocampal neurogenesis and in motivational aspects to escape from an aversive environment in male mice.

2. **Abbreviated Title**
Doublecortin-like in neurogenesis

3. **Authors and Affiliations**
Dirk-Jan Saaltink[1], E.W. van Zwet[2] and Erno Vreugdenhil[1]
1. Department of Cell and Chemical Biology, Leiden University Medical, Center, Leiden, The Netherlands
2. Department of Biomedical Data Sciences

4. **Authors Contributions**
DJS and EV designed Research; DJS performed Research; EWvZ performed statistical analysis; DJS and EV wrote the paper

5. **Correspondence should be addressed to**

Erno Vreugdenhil, Department of Cell and Chemical Biology, Section Neurophysiology Leiden University Medical Center, Leiden, The Netherlands.

Tel: +31-71-526-9756.

E-mail: ernovreugdenhil@lumc.nl

6. **Number of figures: 6**
7. **Number of Tables: none**
8. **Number of Multimedia: none**
9. **Number of words in Abstract: 212**
10. **Number of words for Significance Statement: 115**
11. **Number of words in Introduction: 601**
12. **Number of words in Discussion: 1512**

13. **Acknowledgements**
The authors thank Eva Naninck, Maryse Karsten and Sander Griepsma for technical assistance.

14. **Conflict of interest:** The authors report no conflict of interest.
15. **Funding sources:** This work was supported by Top Institute Pharma (project T5-210), The Netherlands.

Doublecortin-like is implicated in adult hippocampal neurogenesis and in motivational aspects to escape from an aversive environment in male mice.

ABSTRACT

Doublecortin-like (DCL) is a microtubule-associated protein that is highly homologous to doublecortin and is crucially involved in embryonic neurogenesis. Here, we have investigated the in vivo role of DCL in adult hippocampal neurogenesis by generating transgenic mice producing inducible shRNA molecules that specifically target DCL but no other splice-variants produced by the DCLK gene.

DCL knockdown resulted in a significant increase in the number of proliferating $BrdU^+$ cells in the subgranular zone one day after BrdU administration. However, the number of surviving newborn adult NeuN+/$BrdU^+$ neurons are significantly decreased when inspected 4 weeks after BrdU administration suggesting a blockade of neuronal differentiation after DCL-KD. In line with this, we observed an increase in the number of proliferating cells, but a significant decrease in post mitotic DCX+ cells that are characterized by long dendrites spanning all dentate gyrus layers. Behavioural analysis showed that DCL-KD strongly extended the escape latency of mice on the circular hole board but did not affect other aspects of this behavioural task.

Together, our results indicate a function for DCL in adult neurogenesis and in the motivation to escape from an aversive environment. In contrast to DCX, its pivotal role in the maturation of post-mitotic neuronal progenitor cells marks DCL as a genuine adult neurogenesis indicator in the hippocampus.

Significant statement

Both the doublecortin and the doublecortin-like kinase (DCLK) 1 gene are crucial for embryonic neurogenesis. The genomic organization of the DCLK I gene is complex with 20 exons that produces multiple splice variants that are derived from two independent promoters. Whether or not the DCLK1 gene and, if so, which splice variant is involved in adult neurogenesis in the hippocampus is presently unknown. We have investigated specifically the role of one DCLK1 splice-variant, doublecortin-like (DCL) that shares a high level of homology with doublecortin in both sequence identity and length, in hippocampal neurogenesis. Our data indicate a pivotal role for DCL in adult hippocampus neurogenesis, which is associated with a change in hippocampal memory performance.

Introduction

The doublecortin (DCX) gene family members are involved in structural plasticity and a rapid adaption of cellular shape (for review see (Reiner et al., 2006). Mutations in the archetypical member of the family, the *doublecortin* (DCX) gene, have been associated with the doublecortex syndrome, which is characterized by aberrant migration of neuroblasts during embryonic development (Francis et al., 1999; Gleeson et al., 1998). Since then, DCX has been extensively used as a marker in the adult central and peripheral nervous system for neurogenesis (see e.g. Sorrells et al., 2019) and for migrating neuronal progenitor cells (Mauffrey et al., 2019). Proteins encoded by this family are microtubule-associated proteins (MAPs) characterized by a-typical microtubule (MT) binding domains, called DC domains.

Another well-characterized member is the doublecortin-like kinase-1 (DCLK1) gene that, like DCX, is necessary for proper neuronal development. Interestingly, like DCX knockout mice, DCLK1 knockout mice also lack a clear phenotype (Deuel et al., 2006) but DCLK/DCX double knockout mice display profound disorganized cortical layering and a disrupted hippocampal structure, suggestive of a compensatory role for the DCLK1 gene in the migration of neuronal progenitor cells during embryogenesis (NPCs; (Deuel et al., 2006;Koizumi et al., 2006). In addition, products of the DCLK1 gene regulate dendritic development *in vitro*, which has been linked with microtubule-guided transport by DCLK1 interaction with the motor protein kinesin-3 (Lipka et al, 2016; Liu et al., 2012; Shin et al., 2013).

The DCLK gene encodes multiple splice-variants encoding proteins containing DC domains and Ser/Thr kinase domains, such as DCLK-long, or Ser/Thr kinase domains only, like DCLK-short (for review see Dijkmans et al., 2010). In addition, the DCLK gene encodes one splice variant called doublecortin-like (DCL), that lacks a kinase domain and is highly homologous to DCX over its entire length (Vreugdenhil et al., 2007). During embryonic development, DCL functions as a microtubule stabilizing protein of mitotic spindles in vitro and in vivo (Vreugdenhil et al., 2007).

Both DCX and DCL are also expressed in the adult brain. Consistent with a function for DCX in

98 the migration of neuronal progenitor cells, profound DCX expression occurs in well-established
99 neurogenic areas in the adult brain (Brown et al., 2003;Couillard-Despres et al., 2005). DCX+
100 neuroblasts are well-studied in the subgranular zone (SGZ) of the dentate gyrus where
101 approximately 20% of the DCX+ cells are proliferating neuronal progenitor cells (NPC's), while
102 the remaining 80% are post mitotic NPC's and/or neuroblasts (Plumpe et al., 2006;Walker et al.,
103 2007). Surprisingly, DCX seems dispensable for the migration and maturation of (NPC's) and
104 neuroblasts (Merz and Lie, 2013), suggesting that DCL, which is co-expressed with DCX in the
105 SGZ (Saaltink et al., 2012), is sufficient for adult neurogenesis to occur in the dentate gyrus.

106 Although a role for DCL and the DCLK1 gene in embryonic neurogenesis seems evident (Deuel et
107 al., 2006;Koizumi et al., 2006;Shu et al., 2006;Vreugdenhil et al., 2007), its functional role in adult
108 neurogenesis remains elusive. To address this role, we have generated inducible DCL-shRNA
109 mice to knockdown DCL in vivo. As neurogenesis is well-established in the dentate gyrus and
110 DCX and DCL expression is restricted to progenitor cells in the SGZ (Saaltink et al., 2012), we
111 have focused on this neurogenic area of the hippocampus. Furthermore, the cognitive
112 performance after DCL knockdown was studied using the CHB paradigm. We report here that
113 inducible knockdown of DCL leads to a dramatic reduction of post-mitotic DCX-positive cells. In
114 addition, impaired neurogenesis does not affect spatial memory formation. However, DLC
115 knockdown leads to a significant increase in the time to escape from the CHB suggesting a subtle
116 role for DCL in context discrimination.

117

Methods

Animals and animal experimentation

Transgenic male mice were obtained from TaconicArtemis GmbH (Köln, Germany). These mice contain an inducible and reversible shRNA expression system (Seibler et al., 2007), which we called DCL-KD mice. The following hairpin sequences targeting the 3'-UTR region of the mRNA encoding DCL (see Fig. 1A) were cloned into the Taconic Artemis system as described previously (Seibler et al., 2007):

5'- TCCC GCTGGTCATCCTGCATCTTGT **TTCAAGAGA** ACAAGATGCAGGATGACCAGC TTTTTA -3'

3'- CGACCAGTAGGACGTAGAACA **AAGTTCTCT** TGTTCTACGTCCTACTGGTCG AAAAATGCGC -5'

Transgenic males were the founders of our heterozygous outbred colony with B6129S6F1 mice. In all our experiments we used males. The shRNA system was induced by doxycycline (dox) via dox containing food pellets (Dox Diet Sterile S3888, 200mg/kg, BioServ, New Jersey, USA). Animals were put for 4 weeks on dox diet (ad libitum) before they were used for any experiment. As control, we used non-induced TG animals that were fed on identical control diet without dox (S4207, BioServ, New Jersey, USA). As tetracycline-based antibiotics alter mitochondrial function, cell metabolism, cell proliferation and survival (Ahler et al., 2013; Chatzispyrou, Held, Mouchiroud, Auwerx, & Houtkooper, 2015; Luger et al., 2018), we used two additional control groups: wildtype littermates fed with chow and fed with dox containing food pellets.

Tissues are obtained from transgenic DCL-KD mice and wildtype littermates born in our animal facility. After dox induction animals were decapitated and brains were quickly removed for dissection of olfactory bulb and hippocampus. Tissue for qPCR was put into RNA*later*® Solution (Applied Biosystems, The Netherlands) and kept at 4°C for a day and stored at -20°C for later use. Tissue for Western Blot analysis was identically dissected, snap-frozen and stored at -80°C for later use.

All experiments were approved by the local committee of Animal Health and Care and performed in compliance with the European Union recommendations for the care and use of laboratory animals.

RNA isolation

Total RNA was extracted using Trizol (Invitrogen, The Netherlands) and checked for concentration and purity using a Nanodrop ND-1000 spectrometer (Thermo Scientific, USA). RNA integrity was checked using RNA nano labchips in an Agilent 2100 Bioanalyser (Agilent Technologies, Inc, USA).

To remove genomic DNA, 1µg RNA of each sample was treated with DNAse Amplification Grade (Invitrogen, The Netherlands) and diluted with DEPC-MQ to 50ng/µl RNA. From this purified RNA, cDNA was generated using Biorad iScript cDNA synthesis kit (Biorad, The Netherlands).

shRNA detection

shRNA targeting DCL was measured using a custom designed Taqman microRNA assay on a ABI 7900HT fast real time PCR system (Applied Biosystems, The Netherlands). Specific primers were designed to detect anti-DCL shRNA (ACAAGAUGCAGGAUGACCAGC). For mouse tissue, snoRNA-202 was used as reference gene and the data was analyzed using the ΔΔCt method (Livak and Schmittgen, 2001).

Western blot analysis

Tissue was solubilised in lysis buffer (1% Tween-20, 1% DOC, 0,1% SDS, 0,15M NaCl and 50 mM Tris pH 7,5) and centrifuged at max speed (14000rpm) for 10 minutes. The protein concentration of the supernatant was measured using the pierce method (Pierce® BCA Protein Assay Kit, Thermo Scientific, Etten-Leur, The Netherlands). Equal amounts of protein (2 µg cell lysate) were separated by SDS-PAGE (10% acrylamyde) and transferred to immobilon-P PVDF membranes (Millipore).

Blots were incubated in a blocking buffer (TBST, Tris-buffered saline with 0.2% Tween 20, with 5% low-fat milk powder) for 60 minutes and then incubated in fresh blocking buffer with primary antibodies as described (Saaltink et al., 2012) anti-DCL, 1 : 2000; monoclonal α-tubulin DM1A, 1:10000; Sigma–Aldrich, The Netherlands) for another 60 minutes. After a five minutes wash (3x) with TBST, horseradish peroxidase-conjugated secondary antibodies were added in TBST. After treatment with 10 ml luminol (200ml 0,1M Tris HCL, pH8. 50 mg sodium luminol, 60 µl 30% H_2O_2), 100 µl Enhancer (11mg para-hydroxy-coumaric acid in 10 ml DMSO) and 3 µl H_2O_2 protein detection, was performed by ECL™ western blotting analysis system (Amersham Pharmacia Biotech, Freiburg, Germany).

The developed films were scanned at a high resolution (13200 dpi) and gray-values were measured using Image-J. α-tubulin expression was used to correct for the amount of protein for each sample.

Histology

BrdU treatment

To test whether DCL knockdown had an effect on adult neurogenesis, BrdU was used to label proliferating cells. In the first experiment, wildtype and transgenic animals of 6 weeks old were put on a dox or control diet (n=6 per group). After 4 weeks, mice received a single intraperitoneal injection with BrdU (200 mg/kg BrdU dissolved in 0.9% saline, Sigma Aldrich). After 24 hours the animals were decapitated and prepared for immunohistochemistry as described previously (Saaltink et al., 2012). In a second experiment, animals received a similar diet described above for 4 weeks. Subsequently, intraperitoneal BrdU (100 mg/kg BrdU dissolved in 0.9% saline, Sigma Aldrich) was administrated for 4 consecutive days. The animals were kept on the experimental diet for another 4 weeks were after the animals were decapitated and prepared for immunohistochemistry as described before.

Immunohistochemistry

To measure proliferation, BrdU was visualized with 3,3'-Diaminobenzidine (DAB) as previously described (Heine et al., 2004). In short, free-floating sections were incubated in 0.5% H_2O_2 to block endogenous peroxidase. Subsequently, the sections were incubated in mouse α-BrdU primary antibody (clone: BMC9318, Roche Diagnostics, The Netherlands, 1:1000 overnight) and subsequently in sheep α mouse biotinylated secondary antibody (RPN1001, GE Healthcare, Germany, 1:200 for 2 hrs); both antibodies diluted in 0.1% Bovine Serum Albumin (BSA; sc-2323; Santa Cruz Biotechnology), 0.3% TX-100 and 0.1M phosphate buffer. To amplify the signal, a VectaStain Elite avidin-biotin complex (ABC) Kit (Vector Laboratories, Brunschwig Chemie, Amsterdam, The Netherlands, 1:800 for 2 hrs) and tyramide (TSA™ Biotin System, Perkin-Elmer, Groningen, The Netherlands, 1:750 for 45 minutes) were used. Thereafter, sections were incubated with DAB (0.5 mg/ml), dissolved in 0.05M tris-buffer (TB) with 0.01% H2O2 for 15 minutes. Sections were air-dried and counterstained with haematoxylin, dehydrated and cover slipped with DPX (MerckMillipore, Darmstadt, Germany).

To analyze cell survival, chicken α-BrdU (ab92837, Abcam, Cambridge, UK, 1:1000) and mouse α-NeuN (MAB3777, Millipore Billerica, MA, 1:200) were visualized with fluorescent secondary antibodies (Alexa Fluor®488, goat α-chicken and Alexa Fluor®594 donkey α-mouse, Invitrogen, Breda, The Netherlands).

To analyze the immature cell population in the dentate gyrus, DCX was visualized with DAB as previously described (Oomen et al., 2007). Briefly, free-floating sections were incubated in 0.5% H_2O_2 in 0.05 M tris-buffered saline (TBS; pH 7.6) to block endogenous peroxidise. Before primary antibody incubation, the sections were blocked in 2% low-fat milk powder (Elk, Campina, The Netherlands) in TBS for 30 minutes. Sections were incubated in goat α-DCX (sc-8066; Santa Cruz Biotechnology, Santa Cruz, CA, 1:800 overnight) and subsequently in biotinylated donkey α-goat (sc-2042; Santa Cruz Biotechnology, Santa Cruz, CA, 1:500) for 2 hrs. Both antibodies were diluted in TBS with 0.25% gelatine and 0.1% TX-100. To amplify the signal a VectaStain Elite avidin-biotin complex (ABC) Kit and tyramide were used. Incubation of 15 minutes in DAB (0.5

mg/ml), dissolved in 0.05M tris-buffer (TB) with 0.01% H2O2 finished the staining. Sections were air dried and counterstained with haematoxylin, dehydrated and cover slipped with DPX.

Cell counting

Every tenth section of the collected material (1 series out of 10) was stained according the procedures described above. In case of proliferation, all BrdU positive cells in the dentate gyrus were estimated by counting the cells within this series and multiply this with 10. For cell survival, BrdU and NeuN double positive cells were counted. To analyze the immature population of newborn neurons a distinction based on the dendritic morphology was made between three types of DCX positive cells (Plumpe et al., 2006). We categorized DCX positive cells in proliferative stage (type 1, short of no processes), intermediate stage (type 2, medium processes) and post mitotic stage (type 3, strong dendrites with branches). For all three experiments, the total amount of cells in each section was multiplied by 10.

Circular hole board (CHB)

Apparatus

The CHB paradigm (CHB, Fig. 4) was performed as described previously (Dalm et al., 2009). In short, a round Plexiglas plate (diameter: 110 cm) with 12 holes (diameter: 5 cm) was situated 1 meter above the floor (Fig. 4C). The holes were connected to an s-shaped tube of 15 cm length. Beneath the tube, the home cage was placed such to enable the animal to leave the plate and enter its cage. At 5 cm depth, the holes could be closed by a lid. One week before the experimental procedure, the animals were trained to climb through the tunnel 3 times.

Procedure

At day 1, each mouse started with a Free Exploration Trial (FET) of 300 sec. All holes were closed by a lid and the mouse was allowed to move freely over the board. Seven days after the FET the animals proceeded with a 4 days training session with two trainings a day (120 sec) in

which the mice learned to find the exit to their home cage. One day after the training sessions the animals were once again placed on the board for a FET of 120 sec.

Behavioural assessments

Video recorded behaviour was automatically analyzed (distance moved, velocity) by Ethovision software (Noldus BV, Wageningen, The Netherlands) combined with manually collected data like hole visits, latency to target and the escape latency. For the latency to target (also mentioned as first visit latency) the time was measured between the start of the trial until placing the nose in the correct hole for the first time. For escape latency the time was measured between the start of the trial until entering the cage. For the automatically analysed parameters mean distance and mean velocity the time was taken between the start of the trial until escape from the board or, if this did not happen, the end of the trial (after 120 sec).

Statistics

Results are expressed as mean ±S.E.M. and two-way ANOVA was performed using SPSS statistical software. Behavioural data is tested with a General Linear Model (GLM) for repeated measurements in SPSS statistical software version 20 (IBM, SPSS Inc. Chicago,IL).

Results

Generation of DCL-KD mice.

To create an inducible DCL-specific knockdown mouse, we designed a shRNA molecule that targets the 3'-UTR of the DCL mRNA that is absent in other splice-variants of the DCLK gene (see Fig. 1A) and has no significant homology with other members of the DCX family. This DCL-specific shRNA was used to generate doxycycline-inducible knockdown mice according standard procedures (Seibler et al, 2007). No obvious phenotypic differences were observed with respect to weight, breeding and behaviour in the transgenic DCL-KD mice compared to their littermate WT controls. We checked the expression of DCL-targeting shRNA with or without dox administration by a DCL-specific custom-made qPCR approach. As expected, no shRNA-DCL expression was detected in WT littermate mice (data not shown). Strong hairpin induction was found in both hippocampus and olfactory bulb of DCL-KD mice (in both cases; student's t-test, n=4, two-tailed, *** $p < 0.0001$). Compared to transgenic littermates on control diet, a 10 (Hi) and 25 (OB) fold higher expression of shRNA was measured in transgenic animals on dox diet (see Fig. 1D). To investigate specificity of the DCL shRNA, we analyzed the expression of all DCLK1 gene derived proteins by Western blot analysis. DCL protein levels were reduced to 25% after doxycycline administration in both hippocampus and olfactory bulb (Fig. 1E) while the expression levels of other DCLK1 gene-derived proteins were not affected (Fig. 1B). To check for possible fluctuations in DCL expression during neuronal embryogenesis and early postnatal development, a neuronal developmental time-window depending critically on proper expression of DCLK1 gene expression, we inspected DCL expression at embryonic day 14 and postnatal day 1 and 4 by western blot analysis. We found no significant differences in DCL protein levels in DCL-KD animals compared to their littermate WT controls. Together, we concluded that we generated a reliable mouse model with inducible DCL-specific knockdown.

DCL knockdown stimulate proliferation but reduces survival of NPCs.

During embryonic development and in cell lines, the DCLK1 gene has been implicated in the formation of mitotic spindles and proliferation of NPCs and in survival of neuroblasts (Verissimo et al., 2010;Verissimo et al., 2013;Vreugdenhil et al., 2007). Therefore, to investigate the role of the DCL splice-variant in proliferation and survival of adult hippocampal NPCs in vivo, we administered the proliferation marker BrdU (Fig. 2B,C and E) to DCL-KD and WT mice and sacrificed these animals after 24 hrs (proliferation) and after 4 weeks (survival). For proliferation, a two-way ANOVA revealed a significant effect ($F(3)=6.079$, $p= 0.004$) with an significant interaction between genotype and diet ($p=0.043$). Pairwise comparisons using t-tests with pooled standard deviation (SD) showed that the number of BrdU positive cells in DCL-KD animals was significantly increased compared to WT animals on dox diet and DCL-KD and WT animals on control diet (respectively $p=0.0056$, $p=0.0022$ and $p=0.0017$, see Fig. 2A). Furthermore, in transgenic DCL-KD mice, the average effect of dox on the outcome BrdU+ NPCs was 987.3 cells (95% confidence interval (CI): 401.7 to 1573, $p=0.00224$; degrees of freedom (df): 19, see Fig. 2A). We measured the survival of newborn NPC's using BrdU in combination with the adult neuron marker NeuN (see Fig. 2D-F). A two-way ANOVA did not show a significant effect ($F(3)=2.77$, $p=0.07$). However, in the doxycycline fed group, pairwise comparison using t tests with pooled SD showed a significant difference between DCL-KD and WT animals ($p=0.01$, see Fig. 2C). In transgenic DCL-KD mice, the average effect of dox on the outcome NeuN/BrdU+ neurons was -127.6 cells (CI 95%: -323.7 to 68.6, $p=0.188$; df: 18, see Fig. 2C). Proliferation and cell survival in wildtype animals were similar as in non-induced transgenic animals. Together, this dataset suggested that proper DCL expression is necessary for NPC survival in the dentate gyrus of the hippocampus.

To investigate the role of DCL in neurogenesis in more detail, we labelled neuronal progenitor cells with DCX, a well-established marker for neurogenesis (Brown et al., 2003). The expression of DCX was restricted to three types of proliferating neuronal precursor cells with no or short processes (here called type 1) or medium processes reaching the molecular layer of the dentate

gyrus (here called type 2) and post-mitotic neuroblasts characterized by elongated dendrites branching into the granule cell layer and molecular layer (here called type 3; categorized after Oomen et al., 2010;Plumpe et al., 2006). Two-way ANOVA testing showed a significant effect in the type 1 and 3 DCX-positive cells (respectively $F(3)=3.377$, $p=0.04$, and $F(3)=3.473$, $p=0.04$). Pairwise comparisons using t-tests with pooled SD revealed that DCL-KD animals had significantly more type 1 DCX^+ cells compared to WT animals on dox diet and DCL-KD and WT animals on control diet (respectively $p=0.03$, $p=0.04$ and $p=0.02$, see Fig. 3E). The average effect of dox in DCL-KD mice on the outcome type 1 DCX^+ NPCs was 2829.4 cells (95% CI: 157.0 to 5501.8, $p=0.039$; df: 19, see Fig. 3A and E). The same pairwise comparison for type 3 cells showed that DCL-KD animals on dox diet have significantly less type 3 cells compared to WT animals on dox diet and DCL-KD and WT animals on control diet (respectively $p=0.03$, $p=0.04$ and $p=0.02$, see Fig. 3B and G). In transgenic DCL-KD mice, the average effect of dox on the outcome type 3 DCX^+ NPCs was -339.2 cells (CI 95%: -665.5 to -12.8, $p=0.042$; df: 19, see Fig. 3B and G). A two-way ANOVA did show that there is no effect on type 2 cells between the 4 groups ($F(3)=1.824$, $p=0.18$, see Fig. 3F). In line with this, in transgenic mice, the effect of dox on the outcome type 2 DCX^+ NPCs was -1694.6 cells (CI 95%: -3553.7 to 164.5, $p=0.072$; df:19, see Fig 3D and F). Thus, DCL knockdown specifically increased the number of mitotic type 1 cells and reduced the number of post mitotic type 3 cells.

DCL-knockdown mice exhibit increased latency to escape from the CHB.

Numerous studies indicated that aberrant neurogenesis in the adult hippocampus is associated with disease-associated impaired learning and memory formation (see e.g. Clelland et al., 2009;Fitzsimons et al., 2013;Sahay et al., 2011); for reviews see (Petrik et al., 2012;Samuels and Hen, 2011). To investigate possible functional consequences of DCL-KD-induced aberrant neurogenesis, we used the CHB paradigm, a behavioural task aiming to study hippocampal memory performance.

Four groups (N=16 each), transgenic mice with and without dox and their wildtype littermate controls were subjected to 8 training sessions during 4 consecutive days followed by a free exploration trial with closed exit hole (probe trial: PT; see Fig. 4). DCL knockdown had no effect on the parameters 'latency to, (two-way ANOVA $F(1)=0.744$, $p=0.392$, Fig. 5B) and 'errors to target' (two-way ANOVA, $F(1)=2{,}222$, $p=0.141$, fig. 5D) measured during the probe trial. All four groups of mice showed a similar decrease over 4 training days in latency to target (two-Way ANOVA for repeated-measures , $F(3)=39{,}521$, $p<0.001$, Fig. 5A) and errors to target (two-Way ANOVA for repeated-measures, $F(3)=13.230$, $p<0.001$, Fig 5C) suggesting that both groups learned the task equally well. indicating that DCL knockdown does not affect spatial learning parameters in the CHB task. However, surprisingly, we observed a highly significant effect on escape latency. All animals showed a learning curve over the four consecutive days ($F(3)=11.859$, $p<0.005$) and for each test within a day ($F(1)=57.136$, $p<0.005$), but overall there is no interaction effect between gene and diet (Two-Way ANOVA for repeated-measures, $F(3)=1.731$, $p=0.171$, Fig. 6A). However, DCL-KD animals had a significant longer escape latency at each first test of a new day (T3, T5 and T7, One-way ANOVA, $F(3)=12.574$, $P<0.005$, Fig 6A). whereby DCL-KD animals exhibited a strong delay in leaving the board after finding the exit hole, to their home cage. This finding was supported by the longer moved distance (Two-Way ANOVA, $F(1)=4.366$, $p=0.041$, Fig. 6C), and the higher number of animals that failed to reach the target (fig. 6B). This suggested that DCL-KD animals were less motivated to escape from an aversive environment.

Discussion

Here we show that DCL is implicated in adult hippocampal neurogenesis. Knockdown of DCL leads to a significant increase in the number of proliferating cells in the subgranular zone one day after BrdU administration. However, the number of newborn adult NeuN+ cells are significantly decreased when studied 4 weeks after BrdU administration suggesting a suppression of neuronal development after DCL-KD. In line with this, the number of post-mitotic DCX+ NPC's are dramatically reduced. As other splice-variants of the DCLK1 gene are unaffected and expressed at normal levels, our results demonstrate a role for DCL in the differentiation of newborn neurons that is not compensated for by other DCLK splice variants or other members of the DCX gene family including DCX. Strikingly, DCL-KD strongly reduces the escape latency of mice on the CHB but does not affect other aspects of this behavioral task. Together, our analysis indicates a key role for DCL in cell proliferation, migration and maturation. DCL is furthermore involved in motivational aspects to escape from an aversive environment.

DCL-KD leads to a significant decrease in the number of post-mitotic NeuN+/BrdU+ cells while the number proliferating BrdU+ cells are increased. These data suggest involvement of DCL in cell proliferation and subsequent survival of new born neurons. Indeed, the DCLK1 gene has been shown to regulate dendritic development (Lipka et al., 2016; Liu et al., 2012; Shin et al., 2013) and the form of mitotic spindles in embryonic NPC's and neuroblasts in vitro and in vivo (Shu et al., 2006;Vreugdenhil et al., 2007). In *C. elegans*, the orthologue of the DCLK1 gene, zyg-8, regulate asymmetric division of fertilized eggs by controlling the length of mitotic spindles (Gonczy et al., 2001). Also in mammals, a correct positioning of mitotic spindles in radial glia cells has been associated with proper differentiation of the resulting neuronal daughter cells (Lancaster and Knoblich, 2012). Initial neuro-epithelial cell division may occur symmetrical and subsequently, neuronal progenitor cells, i.e. radial glia cells, are believed to divide asymmetrically during embryonic neurogenesis. In analogy with such a proliferation and differentiation scheme, type 1 and type 2 DCX+ cells may represent symmetric dividing

progenitor cells in the adult SGZ while type 3 post-mitotic DCX+ cells may be the result of an a-symmetric cell division requiring functional DCL. Additionally, The DCLK gene has been shown to be a pro-survival gene in neuroblastoma cells (Kruidering et al., 2001) and is a target for pro-apoptotic enzymes such as caspases and calpain (Burgess and Reiner, 2001;Kruidering et al., 2001). Moreover, DCLK knockdown by RNA-interference technology leads to the activation of a pro-apoptotic program in neuroblastoma cells (Verissimo et al., 2010) and to a reduction of neuronal progenitor cells during neocortical development in vivo (Vreugdenhil et al., 2007). As the shRNA molecule targets DCL specifically, leaving other DCLK splice-variants unaltered, our data indicate a role for DCL in the transition and survival of proliferating to post-mitotic DCX+ NPCs.

Knockdown of DCL leads to a phenotypic change of DCX+ cells. This finding suggests that both DCL and DCX are expressed in the same NPC's in the subgranular zone of the dentate gyrus. In line with DCL/DCX colocalization are the phenotypic analysis of Dcx/Dclk1 double knockouts mice showing functional redundancy during hippocampal lamination (Tanaka et al., 2006). Also, gene expression profiling of human primary neuroblasts clearly demonstrate coexpression of DCX and DCL (Verissimo et al., 2010). Moreover, our previous immunohistochemical experiments also showed DCX-DCL co-localization in NPC's in the subgranular of the dentate gyrus and in neuroblasts in the rostral migratory stream (Saaltink et al., 2012). Thus, it seems that colocalization of DCX and DCL are required for proper neuronal migration and differentiation. However, at the subcellular level it seems that DCX and DCL are located at different locations with prominent DCX signals that follows projections forming a dendritic blueprint (see e.g. Fig. 3A) while DCL mainly appeared in speckles at specific dendritic hotspots (Saaltink et al., 2012). Also, detailed immunohistochemical analysis during embryonic development shows spatiotemporal differences in expression of DCX and DCL (Boekhoorn et al., 2008). Thus, it seems that DCL and DCX have different subcellular functions in within a cell. However, overexpression or microRNA-mediated DCX knockdown did not alter migration or morphological maturation of NPC's in the SGZ suggesting that DCX is dispensable for proper

412 hippocampal neurogenesis (Merz and Lie, 2013). Thus, it seems that DCX and DCL function
413 differently in NPCs with an unique key role for DCL in adequate morphological maturation.

414 Previously, we reported a role for DCL in intracellular transport of the glucocorticoid receptor
415 (Fitzsimons et al., 2008), the main mediator of the stress response and a crucial molecule for the
416 migration and maturation of new born neurons (Fitzsimons et al., 2013). shRNA mediated GR
417 knockdown leads to hyperactive neuronal migration and maturation. Since DCL is directly
418 involved in intracellular GR transport, one might expect similar hyperactive neurogenesis after
419 DCL knockdown. However, activated GR's are associated with reduced neurogenesis (Gould et
420 al., 1998) and the increased proliferation after DCL knockdown fits into the picture of reduced
421 GR activity. The strongly reduced migration and maturation of NPC's after DCL knockdown is
422 opposite to GR knockdown mediated hyperactive development and suggest that DCL serves
423 more functions beside GR transport. One such function may be mediated by an interaction with
424 members of the kinesin family as DCLK guides kinesin-3 (Lipka et al., 2016) and kinesins have
425 been implicated in the mechanisms underlying asymmetric cell divisions of neuronal progenitor
426 cells (Hakanen et al, 2019; McNeely et al., 2017).

427 DCL knockdown results in aberrant adult neurogenesis but does not affect spatial learning on
428 the CHB. This finding is somewhat unexpected as several studies reported association of
429 reduced neurogenesis and impaired spatial and contextual learning in several behavioral tasks
430 such as contextual fear conditioning (Seo et al, 2015; Saxe et al., 2006) and, similar as the CHB,
431 the Barnes maze (Imayoshi et al., 2008). However, these findings were not reproduced by
432 numerous other investigators (Martinez-Canabal et al., 2013; Meshi et al., 2006; Shors et al.,
433 2002; Zhang et al., 2008). For example, even complete ablation of neurogenesis in cyclin D2
434 knockout mice leads to normal spatial learning and contextual memory formation (Jaholkowski
435 et al., 2009; Jedynak et al., 2012; Urbach et al., 2013). Moreover, addition of new neurons is not
436 necessary for hippocampus-dependent learning (Frankland, 2013) but may be involved in
437 forgetting, although this is dependent on the memory task used and its timing in relation to

neurogenesis (Gao et al., 2018). Recent studies suggest a role for adult neurogenesis in a more subtle cognitive hippocampal function, i.e. pattern separation (França et al, 2017; Clelland et al., 2009; Sahay et al., 2011). Thus, the CHB paradigm may be too robust to find possible cognitive hippocampus-mediated impairments after DCL knockdown. Alternatively, DCL knockdown leads to approximately 75% reduction of adult-born post-mitotic neurons (Fig. 3G), which may be insufficient to detect neurogenesis-related behavioral differences.

Surprisingly, DCL-KD leads to a highly significant increase in the latency to leave the CHB. Possibly, motivation to leave the CHB, might be fear-regulated by the aversive environment created by the board and as such, comparable with context fear conditioning which may be partly regulated by adult neurogenesis (Denny et al., 2012;Drew et al., 2010). Also, this increase in latency is associated with more motor activity with longer moved distances after DCL knockdown, a phenomenon that is also linked to a lesioned hippocampus (Deacon et al., 2002). Alternatively, although DCL has a highly restrictive expression pattern in the hippocampus (Saaltink et al., 2012), we cannot exclude the possibility that other brain areas are involved. In particular, DCL is also highly expressed in the olfactory bulb (OB). Ablation of newly born neurons does not affect olfactory detection levels, however, it might affect downstream processing of odour information (Gheusi et al., 2000; Imayoshi et al., 2008) and as such DCL knockdown might impair olfactory discrimination. Therefore, impaired olfaction might result in impaired recognition of the home cage, which might explain the increased latency to leave the board. However, olfaction is an equally important parameter to learn spatial memory tasks adequately (Machado et al., 2012; van Rijzingen et al., 1995). Moreover, we did not observe any differences, as in the hippocampus, in the form and number of DCX+ cells in the OB (unpublished data) while DCL is also expressed in other brain areas characterized by a high level of neuronal plasticity (Saaltink et al., 2012). Therefore, we favor the hypothesis that the increase in latency is due to impaired structural alterations in the dentate gyrus.

463 We have successfully generated a transgenic animal model to study the role of a specific splice-
464 variant of the DCLK gene, i.e. DCL, without affecting the expression of the other splice-variants
465 DCLK-long and DCLK-short. Using this model, we found that DCL is involved in the transition of
466 proliferating NPCs into post mitotic neuroblasts. Moreover, behavioral studies show that DCL
467 may be involved in motivational aspects to escape from aversive environments. Our model
468 seems a valuable *in vivo* tool to study these areas and the role of DCL therein, in a
469 multidisciplinary fashion.

470

471 **Reference List**

472

473 Ahler E, Sullivan WJ, Cass A, Braas D, York AG, Bensinger SJ, et al. (2013). Doxycycline alters
474 metabolism and proliferation of human cell lines. PloS One, 8(5), e64561.
475 http://doi.org/10.1371/journal.pone.0064561

476 Boekhoorn K, Sarabdjitsingh A, Kommerie H, de PK, Schouten T, Lucassen PJ, Vreugdenhil E
477 (2008) Doublecortin (DCX) and doublecortin-like (DCL) are differentially expressed in the early
478 but not late stages of murine neocortical development. J Comp Neurol 507:1639-1652.

479 Brown JP, Couillard-Despres S, Cooper-Kuhn CM, Winkler J, Aigner L, Kuhn HG (2003) Transient
480 expression of doublecortin during adult neurogenesis. Journal of Comparative Neurology 467:1-
481 10.

482 Burgess HA, Reiner O (2001) Cleavage of doublecortin-like kinase by calpain releases an active
483 kinase fragment from a microtubule anchorage domain. J Biol Chem 276:36397-36403.

484 Chatzispyrou IA, Held NM, Mouchiroud L, Auwerx, J, and Houtkooper RH (2015). Tetracycline
485 antibiotics impair mitochondrial function and its experimental use confounds research. Cancer
486 Research, 75(21), 4446–4449. http://doi.org/10.1158/0008-5472.CAN-15-1626

487 Clelland CD, Choi M, Romberg C, Clemenson GD, Jr., Fragniere A, Tyers P, Jessberger S, Saksida
488 LM, Barker RA, Gage FH, Bussey TJ (2009) A functional role for adult hippocampal neurogenesis
489 in spatial pattern separation. Science 325:210-213.

490 Couillard-Despres S, Winner B, Schaubeck S, Aigner R, Vroemen M, Weidner N, Bogdahn U,
491 Winkler J, Kuhn HG, Aigner L (2005) Doublecortin expression levels in adult brain reflect
492 neurogenesis. Eur J Neurosci 21:1-14.

493 Dalm S, Schwabe L, Schachinger H, Oitzl MS (2009) Post-training self administration of sugar
494 facilitates cognitive performance of male C57BL/6J mice in two spatial learning tasks. Behav
495 Brain Res 198:98-104.

496 Deacon RM, Croucher A, Rawlins JN (2002) Hippocampal cytotoxic lesion effects on species-
497 typical behaviours in mice. Behav Brain Res 132:203-213.

498 Denny CA, Burghardt NS, Schachter DM, Hen R, Drew MR (2012) 4- to 6-week-old adult-born
499 hippocampal neurons influence novelty-evoked exploration and contextual fear conditioning.
500 Hippocampus 22:1188-1201.

501 Deuel TAS, Liu JS, Corbo JC, Yoo SY, Rorke-Adams LB, Walsh CA (2006) Genetic interactions
502 between doublecortin and doublecortin-like kinase in neuronal migration and axon outgrowth.
503 Neuron 49:41-53.

504 Dijkmans TF, van Hooijdonk LW, Fitzsimons CP, Vreugdenhil E (2010) The doublecortin gene
505 family and disorders of neuronal structure. Cent Nerv Syst Agents Med Chem 10:32-46.

506 Drew MR, Denny CA, Hen R (2010) Arrest of adult hippocampal neurogenesis in mice impairs
507 single- but not multiple-trial contextual fear conditioning. Behav Neurosci 124:446-454.

508 Fitzsimons CP, Ahmed S, Wittevrongel CF, Schouten TG, Dijkmans TF, Scheenen WJ, Schaaf MJ, de
509 Kloet ER, Vreugdenhil E (2008) The microtubule-associated protein doublecortin-like regulates
510 the transport of the glucocorticoid receptor in neuronal progenitor cells. Mol Endocrinol 22:248-
511 262.

512 Fitzsimons CP, van Hooijdonk LW, Schouten M, Zalachoras I, Brinks V, Zheng T, Schouten TG,
513 Saaltink DJ, Dijkmans T, Steindler DA, Verhaagen J, Verbeek FJ, Lucassen PJ, de Kloet ER, Meijer
514 OC, Karst H, Joels M, Oitzl MS, Vreugdenhil E (2013) Knockdown of the glucocorticoid receptor
515 alters functional integration of newborn neurons in the adult hippocampus and impairs fear-
516 motivated behavior. Mol Psychiatry 18:993-1005.

517 Francis, F., Koulakoff, A., Boucher, D., Chafey, P., Schaar, B., Vinet, M. C., et al. (1999).
518 Doublecortin is a developmentally regulated, microtubule-associated protein expressed in
519 migrating and differentiating neurons. Neuron 23: 247–256.
520
521 França, T. F. A., Bitencourt, A. M., Maximilla, N. R., Barros, D. M., & Monserrat, J. M. (2017).
522 Hippocampal neurogenesis and pattern separation: A meta-analysis of behavioral data.
523 Hippocampus 27: 937–950.
524
525 Frankland PW (2013) Neurogenic evangelism: comment on Urbach et al. (2013). Behav Neurosci
526 127:126-129.

527 Gao, A., Xia, F., Guskjolen, A. J., Ramsaran, A. I., Santoro, A., Josselyn, S. A., & Frankland, P. W.
528 (2018). Elevation of Hippocampal Neurogenesis Induces a Temporally Graded Pattern of
529 Forgetting of Contextual Fear Memories. J. Neurosc: 38: 3190–3198.
530
531 Gheusi G, Cremer H, McLean H, Chazal G, Vincent JD, Lledo PM (2000) Importance of newly
532 generated neurons in the adult olfactory bulb for odor discrimination. Proc Natl Acad Sci U S A
533 97:1823-1828.

534 Gleeson, J. G., Allen, K. M., Fox, J. W., Lamperti, E. D., Berkovic, S., Scheffer, I., et al. (1998).
535 Doublecortin, a brain-specific gene mutated in human X-linked lissencephaly and double cortex
536 syndrome, encodes a putative signaling protein. Cell: 92: 63–72.
537
538 Gonczy P, Bellanger JM, Kirkham M, Pozniakowski A, Baumer K, Phillips JB, Hyman AA (2001)
539 zvg-8, a gene required for spindle positioning in C-elegans, encodes a doublecortin-related
540 kinase that promotes microtubule assembly. Developmental Cell 1:363-375.

541 Gould E, Tanapat P, Mcewen BS, Flugge G, Fuchs E (1998) Proliferation of granule cell precursors
542 in the dentate gyrus of adult monkeys is diminished by stress. Proceedings of the National
543 Academy of Sciences of the United States of America 95:3168-3171.

544 Hakanen, J., Ruiz-Reig, N., & Tissir, F. (2019). Linking Cell Polarity to Cortical Development and
545 Malformations. Frontiers in Cellular Neuroscience: 13, 244.

546 Heine VM, Maslam S, Joels M, Lucassen PJ (2004) Prominent decline of newborn cell
547 proliferation, differentiation, and apoptosis in the aging dentate gyrus, in absence of an age-
548 related hypothalamus-pituitary-adrenal axis activation. Neurobiol Aging 25:361-375.

549 Imayoshi I, Sakamoto M, Ohtsuka T, Takao K, Miyakawa T, Yamaguchi M, Mori K, Ikeda T, Itohara
550 S, Kageyama R (2008) Roles of continuous neurogenesis in the structural and functional
551 integrity of the adult forebrain. Nat Neurosci 11:1153-1161.

552 Jaholkowski P, Kiryk A, Jedynak P, Ben Abdallah NM, Knapska E, Kowalczyk A, Piechal A,
553 Blecharz-Klin K, Figiel I, Lioudyno V, Widy-Tyszkiewicz E, Wilczynski GM, Lipp HP, Kaczmarek L,
554 Filipkowski RK (2009) New hippocampal neurons are not obligatory for memory formation;
555 cyclin D2 knockout mice with no adult brain neurogenesis show learning. Learn Mem 16:439-
556 451.

557 Jedynak P, Jaholkowski P, Wozniak G, Sandi C, Kaczmarek L, Filipkowski RK (2012) Lack of cyclin
558 D2 impairing adult brain neurogenesis alters hippocampal-dependent behavioral tasks without
559 reducing learning ability. Behav Brain Res 227:159-166.

560 Koizumi H, Tanaka T, Gleeson JG (2006) Doublecortin-like kinase functions with doublecortin to
561 mediate fiber tract decussation and neuronal migration. Neuroscience Research 55:S238.

562 Kruidering M, Schouten T, Evan GI, Vreugdenhil E (2001) Caspase-mediated cleavage of the
563 Ca2+/calmodulin-dependent protein kinase-like kinase facilitates neuronal apoptosis. Journal of
564 Biological Chemistry 276:38417-38425.

565 Lancaster MA, Knoblich JA (2012) Spindle orientation in mammalian cerebral cortical
566 development. Curr Opin Neurobiol 22:737-746.

567 Lipka, J., Kapitein, L. C., Jaworski, J., & Hoogenraad, C. C. (2016). Microtubule-binding protein
568 doublecortin-like kinase 1 (DCLK1) guides kinesin-3-mediated cargo transport to dendrites. The
569 EMBO Journal 35: 302–318.

570 Livak KJ, Schmittgen TD (2001) Analysis of relative gene expression data using real-time
571 quantitative PCR and the 2(-Delta Delta C(T)) Method. Methods 25:402-408.

572 Liu, J. S., Schubert, C. R., Fu, X., Fourniol, F. J., Jaiswal, J. K., Houdusse, A., et al. (2012). Molecular
573 basis for specific regulation of neuronal kinesin-3 motors by doublecortin family proteins.
574 Molecular Cell 47: 707–721.

575 Luger A-L, Sauer B, Lorenz NI, Engel AL, Braun Y, Voss M, et al. (2018). Doxycycline Impairs
576 Mitochondrial Function and Protects Human Glioma Cells from Hypoxia-Induced Cell Death:
577 Implications of Using Tet-Inducible Systems. International Journal of Molecular Sciences, 19(5), 1504.
578 http://doi.org/10.3390/ijms19051504

579 Machado DG, Cunha MP, Neis VB, Balen GO, Colla AR, Grando J, Brocardo PS, Bettio LE, Dalmarco
580 JB, Rial D, Prediger RD, Pizzolatti MG, Rodrigues AL (2012) Rosmarinus officinalis L.
581 hydroalcoholic extract, similar to fluoxetine, reverses depressive-like behavior without altering
582 learning deficit in olfactory bulbectomized mice. J Ethnopharmacol 143:158-169.

583 Martinez-Canabal A, Akers KG, Josselyn SA, Frankland PW (2013) Age-dependent effects of
584 hippocampal neurogenesis suppression on spatial learning. Hippocampus 23:66-74.

585 Mauffrey, P., Tchitchek, N., Barroca, V., Bemelmans, A., Firlej, V., Allory, Y., et al. (2019).
586 Progenitors from the central nervous system drive neurogenesis in cancer. Nature 569: 672–
587 678.

588 McNeely, K. C., Cupp, T. D., Little, J. N., Janisch, K. M., Shrestha, A., & Dwyer, N. D. (2017). Mutation
589 of Kinesin-6 Kif20b causes defects in cortical neuron polarization and morphogenesis. Neural
590 Development 12: 5.

591 Merz K, Lie DC (2013) Evidence that Doublecortin is dispensable for the development of adult
592 born neurons in mice. PLoS One 8:e62693.

593 Meshi D, Drew MR, Saxe M, Ansorge MS, David D, Santarelli L, Malapani C, Moore H, Hen R
594 (2006) Hippocampal neurogenesis is not required for behavioral effects of environmental
595 enrichment. Nature Neuroscience 9:729-731.

596 Oomen CA, Mayer JL, de Kloet ER, Joels M, Lucassen PJ (2007) Brief treatment with the
597 glucocorticoid receptor antagonist mifepristone normalizes the reduction in neurogenesis after
598 chronic stress. Eur J Neurosci 26:3395-3401.

599 Oomen CA, Soeters H, Audureau N, Vermunt L, van Hasselt FN, Manders EM, Joels M, Lucassen PJ,
600 Krugers H (2010) Severe early life stress hampers spatial learning and neurogenesis, but
601 improves hippocampal synaptic plasticity and emotional learning under high-stress conditions
602 in adulthood. J Neurosci 30:6635-6645.

603 Petrik D, Lagace DC, Eisch AJ (2012) The neurogenesis hypothesis of affective and anxiety
604 disorders: are we mistaking the scaffolding for the building? Neuropharmacology 62:21-34.

605 Plumpe T, Ehninger D, Steiner B, Klempin F, Jessberger S, Brandt M, Romer B, Rodriguez GR,
606 Kronenberg G, Kempermann G (2006) Variability of doublecortin-associated dendrite
607 maturation in adult hippocampal neurogenesis is independent of the regulation of precursor cell
608 proliferation. BMC Neurosci 7:77.

609 Reiner O, Coquelle FM, Peter B, Levy T, Kaplan A, Sapir T, Orr I, Barkai N, Eichele G, Bergmann S
610 (2006) The evolving doublecortin (DCX) superfamily. Bmc Genomics 7.

611 Saaltink DJ, Havik B, Verissimo CS, Lucassen PJ, Vreugdenhil E (2012) Doublecortin and
612 doublecortin-like are expressed in overlapping and non-overlapping neuronal cell population:
613 Implications for neurogenesis. J Comp Neurol 520:2805-2823.

614 Sahay A, Scobie KN, Hill AS, O'Carroll CM, Kheirbek MA, Burghardt NS, Fenton AA, Dranovsky A,
615 Hen R (2011) Increasing adult hippocampal neurogenesis is sufficient to improve pattern
616 separation. Nature 472:466-U539.

617 Samuels BA, Hen R (2011) Neurogenesis and affective disorders. Eur J Neurosci 33:1152-1159.

618 Saxe MD, Battaglia F, Wang JW, Malleret G, David DJ, Monckton JE, Garcia ADR, Sofroniew MV,
619 Kandel ER, Santarelli L, Hen R, Drew MR (2006) Ablation of hippocampal neurogenesis impairs
620 contextual fear conditioning and synaptic plasticity in the dentate gyrus. Proceedings of the
621 National Academy of Sciences of the United States of America 103:17501-17506.

622 Seibler J, Kleinridders A, Kuter-Luks B, Niehaves S, Bruning JC, Schwenk F (2007) Reversible
623 gene knockdown in mice using a tight, inducible shRNA expression system. Nucleic Acids Res
624 35:e54.

625 Seo D-O, Carillo M A, Chih-Hsiung Lim S, Tanaka K F, Drew, M R (2015). Adult Hippocampal
626 Neurogenesis Modulates Fear Learning through Associative and Nonassociative Mechanisms. J.
627 Neurosci 35: 11330–11345.

628 Shin E, Kashiwagi Y, Kuriu T, Iwasaki H, Tanaka T, Koizumi H, Gleeson JG, Okabe S (2013)
629 Doublecortin-like kinase enhances dendritic remodelling and negatively regulates synapse
630 maturation. Nat Commun 4:1440.

631 Shors TJ, Townsend DA, Zhao M, Kozorovitskiy Y, Gould E (2002) Neurogenesis may relate to
632 some but not all types of hippocampal-dependent learning. Hippocampus 12:578-584.

633 Shu TZ, Tseng HC, Sapir T, Stern P, Zhou Y, Sanada K, Fischer A, Coquelle FM, Reiner O, Tsai LH
634 (2006) Doublecortin-like kinase controls neurogenesis by regulating mitotic spindles and M
635 phase progression. Neuron 49:25-39.

636 Sorrells S F, Paredes MF, Velmeshev D, Herranz-Pérez V, Sandoval K, Mayer S, et al. (2019).
637 Immature excitatory neurons develop during adolescence in the human amygdala. Nature
638 Commun 10: 2748.

639 Tanaka T, Koizumi H, Gleeson JG (2006) The Doublecortin and Doublecortin-like kinase 1 genes
640 cooperate in murine hippocampal development. Cerebral Cortex 16:I69-I73.

641 Urbach A, Robakiewicz I, Baum E, Kaczmarek L, Witte OW, Filipkowski RK (2013) Cyclin D2
642 knockout mice with depleted adult neurogenesis learn Barnes maze task. Behav Neurosci 127:1-
643 8.

644 van Rijzingen I, Gispen WH, Spruijt BM (1995) Olfactory bulbectomy temporarily impairs Morris
645 maze performance: an ACTH(4-9) analog accellerates return of function. Physiol Behav 58:147-
646 152.

647 Verissimo CS, Elands R, Cheng S, Saaltink DJ, Ter Horst JP, Alme MN, Pont C, van de WB, Havik B,
648 Fitzsimons CP, Vreugdenhil E (2013) Silencing of Doublecortin-Like (DCL) Results in Decreased
649 Mitochondrial Activity and Delayed Neuroblastoma Tumor Growth. PLoS One 8:e75752.

650 Verissimo CS, Molenaar JJ, Meerman J, Puigvert JC, Lamers F, Koster J, Danen EHJ, van de Water
651 B, Versteeg R, Fitzsimons CP, Vreugdenhil E (2010) Silencing of the microtubule-associated
652 proteins doublecortin-like and doublecortin-like kinase-long induces apoptosis in
653 neuroblastoma cells. Endocrine-Related Cancer 17:399-414.

654 Vreugdenhil E, Kolk SM, Boekhoorn K, Fitzsimons CP, Schaaf M, Schouten T, Sarabdjitsingh A,
655 Sibug R, Lucassen PJ (2007) Doublecortin-like, a microtubule-associated protein expressed in

radial glia, is crucial for neuronal precursor division and radial process stability. European Journal of Neuroscience 25:635-648.

Walker TL, Yasuda T, Adams DJ, Bartlett PF (2007) The doublecortin-expressing population in the developing and adult brain contains multipotential precursors in addition to neuronal-lineage cells. Journal of Neuroscience 27:3734-3742.

Zhang CL, Zou Y, He W, Gage FH, Evans RM (2008) A role for adult TLX-positive neural stem cells in learning and behaviour. Nature 451:1004-1007.

Legends

Figure 1: Specific knockdown of DCLK1 splice variant DCL. **A)** Overview of the three most important DCLK1 splice variants and their functional components. The shRNA target sequence resides in the 3'-UTR of DCL mRNA which is absent in DCLK-long and DCLK-short. **B)** Western blot analysis reveals splice variant specific knockdown of DCL in dox induced transgenic (TG) animals compared to dox induced wildtype (WT) animals. DCLK-long and DCLK-short expression is not affected. **C)** Although there is some leakage, this leakage does not affect hippocampal DCL expression during embryonic development. There is no significant difference in DCL expression between non-induced wildtype (WT and transgenic (TG) littermates at embryonic day 14 (ED14) and postnatal day 1 and 3 (PND1 & PND3). **D)** After dox induction, in the hippocampal tissue (Hi) an almost 10-fold higher shRNA expression measured compared to non induced transgenic littermates.(student's t-test, n=4, two-tailed, *** $p < 0.0001$) In the olfactory bulb (OB) a nearly 25-fold higher shRNA expression is measured (student's t-test, n=4, two-tailed, *** $p < 0.0001$). **E)** In both hippocampus (Hi, student's t-test, two-tailed, control n=4, dox n=5, ** $p<0.01$) and olfactory bulb (OB, student's t-test, two-tailed, control n=4, dox n=5, *** $p<0.0001$) DCL protein expression is reduced to 25% after dox induction compared to non induced transgenic littermates.

Figure 2: Adult neurogenesis measurement using BrdU labeling. **A:** 24 hours after a single BrdU injection, a significant (2-way ANOVA, $F(3)= 6.079$, $p=0.004$) with an significant interaction between genotype and diet ($p=0.043$). The number of BrdU positive cells is significantly increased compared to WT animals on dox diet and DCL-KD and WT mice on control diets (respectively $p=0.0056$, $p=0.0022$ and $p=0.0017$; n=6). Effect of dox on DCL-KD mice: 95% CI: 401.7 to 1573, $p=0.0022$). **B:** Examples of hippocampi derived from animals killed 24 hours after BrdU injection. Both sections are stained for BrdU and show mainly BrdU positive cells in the subgranular zone. Tissue is derived from dox induced transgenic animals (dox) and non-induced transgenic littermates (control) **C:** BrdU/NeuN double staining revealed a trend

(F(3)=2.77, p=0.057 2-way ANOVA) in double positive cells in hippocampal dentate gyrus of dox induced transgenic animals (dox, n=5) compared to non-induced transgenic littermates and both WT control groups (control, n=4). In the doxycycline fed group, pairwise comparison using t tests with pooled SD shows a significant difference between DCL-KD and WT animals (p=0.01). Effect of dox on DCL-KD mice: CI 95%: -323.7 to 68.6, p=0.188. **D-F:** Confocal laser scanning microscopy images showing co localization of BrdU (green in D) and NeuN (red in E). Only cells in the dentate gyrus who are double positive (yellow in F) were counted. Scale bar in D-F measures 25µm. Significant differences are indicated with an asterisk. Means are indicated with a black bar.

Figure 3: DCX cell morphology. **A:** DCX expressing cells in the hippocampal dentate gyrus of a transgenic animal on an control diet showing a normal DCX morphology with cell nuclei close to the subgranular zone (SGZ) and dendrites towards the molecular layer (ML). **B:** Hippocampal dentate gyrus of a dox induced transgenic littermate showing aberrant morphology of DCX positive cells. Hardly any DCX positive cell has dendrites in the granular cell layer (GCL) or ML. **C-D:** Close-up of DCX expressing cells in the hippocampal dentate gyrus of a transgenic animal on a control diet (**C**). Several DCX positive cells show dendritic outgrow (arrows) towards the molecular layer which are absent after DCL knockdown (**D**). **E-G:** Number of proliferating type 1, 2 an 3 DCX positive cells in transgenic and WT mice on a control or dox diet. Two-way ANOVA testing shows a significant effect in the type 1 and 3 DCX-positive cells (respectively F(3)=3.377, p=0.04, and F(3)=3.473, p=0.04). Effect of dox on DCL-KD mice: CI95% type 1 cells: 157.0 to 5501.8, p=0.039; CI95% type 2 cells: -3553.7 to 164.5, p=0.072; CI95% type 3 cells: -665.5 to -12.8, p=0.042. Significant differences are indicated with an asterisk. Means are indicated with a black bar. For further details: see main text.

Figure 4: Setup of the CHB experiment. **A:** Animals were put on a dox diet for at least 5 weeks before the CHB was started. **B:** The CHB paradigm started with a free exploration trial (FET). 7 days later the animals followed a training for 4 consecutive days with 2 trials a day. At day 5 the

719 animals were exposed to a probe trial in which the escape hole was closed. **C:** The hole board
720 was equipped with 12 holes. During training, 1 hole (black), by which animals could reach their
721 home cage, was open **D:** Photograph of the CHB setup in the lab.

722

723 **Figure 5:** Spatial parameters measured on the CHB. A: First visit latency. All four groups showed
724 a similar decrease over 4 training days in latency to target (Two-Way ANOVA for repeated-
725 measures, $F(3)=39{,}521$, $p<0.001$). B: probe trial. DCL knockdown had no effect on the
726 parameters 'latency to target' (two-way ANOVA $F(1)=0.744$, $p=0.392$) C: Errors to target. All four
727 groups showed a similar decrease over 4 training days in errors to target (Two-Way ANOVA for
728 repeated-measures, $F(3)=13.230$, $p<0.001$). D: probe trial. DCL knockdown had no effect on the
729 parameters 'errors to target' (two-way ANOVA, $F(1)=2{,}222$, $p=0.141$). For further details: see
730 main text.

731

732 **Figure 6:** Motivational parameters measured on the CHB. **A:** DCL-KD animals showed a
733 significant longer escape latency at each first test of the new day (T3, T5 and T7, One-way
734 ANOVA, $F(3)=12.574$, $p<0.005$). **B:** Percent of animals who did not reach the target within 120
735 seconds. **C:** Mean distance moved during each trial. DCL-KD animals move a significant longer
736 distance (two-way ANOVA $F(1)=4.366$, $p=0.041$). **D:** Average velocity during each trial. DCL-KD
737 animals are significant slower compared to DCL+ animals and WT controls (GML, $F(1)=15.101$,
738 $p=0.001$).

739

740

741

742

743

746 **Figure 1**

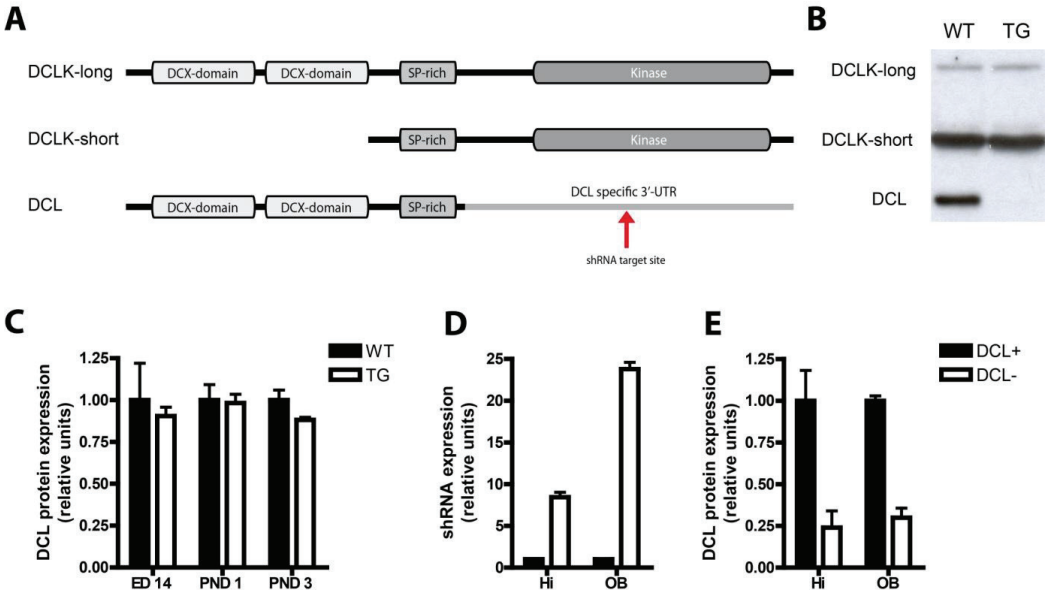

747

748

749 **Figure 2**

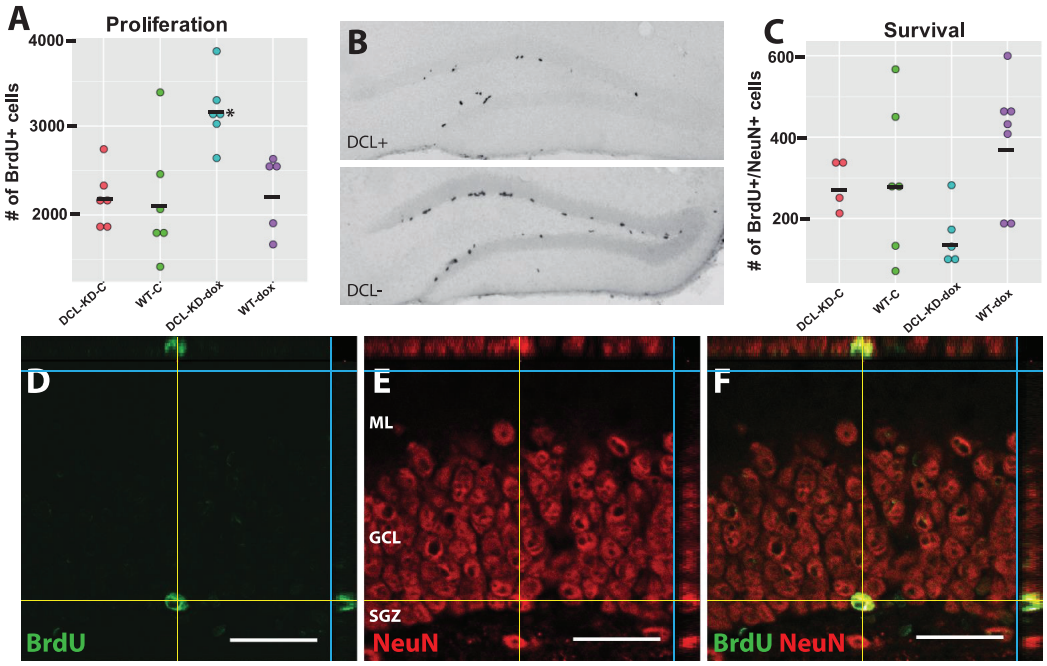

750

751

752 **Figure 3**

753

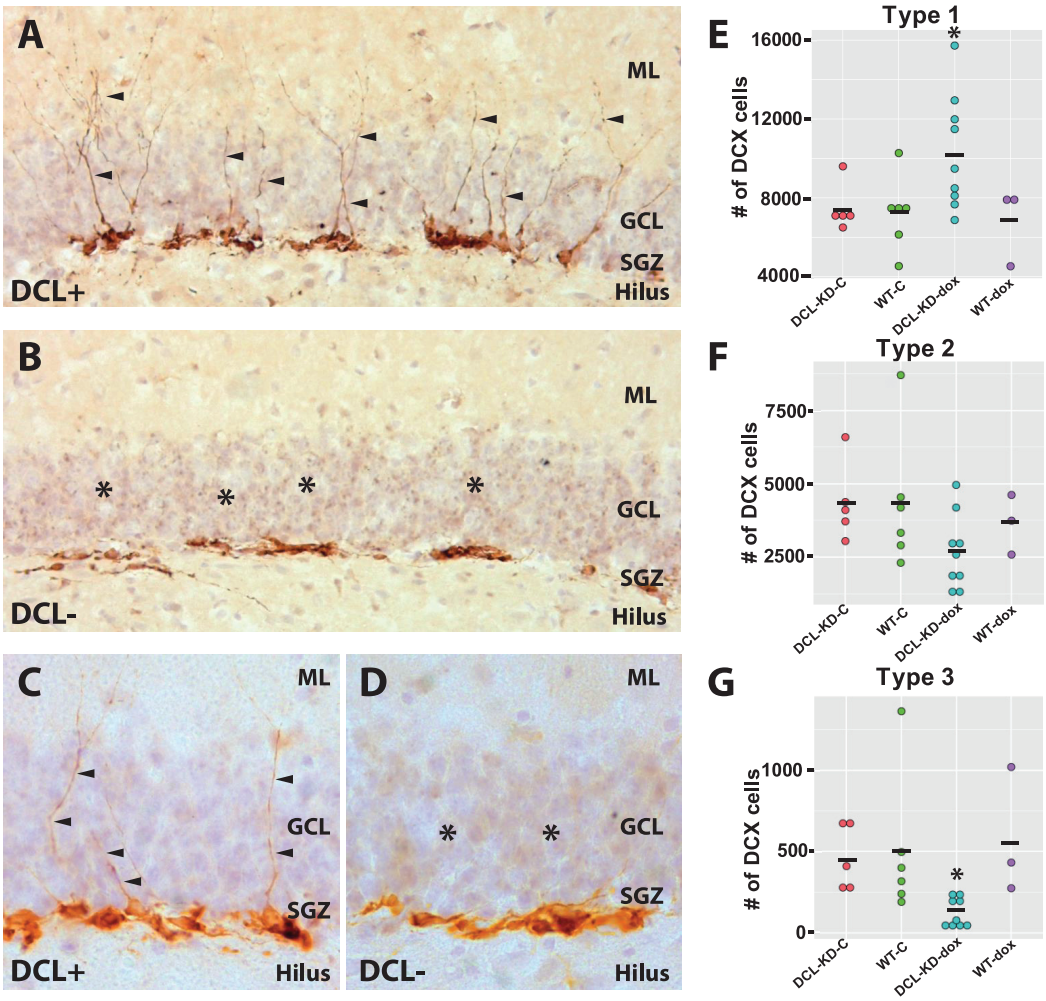

754

755

Figure 4

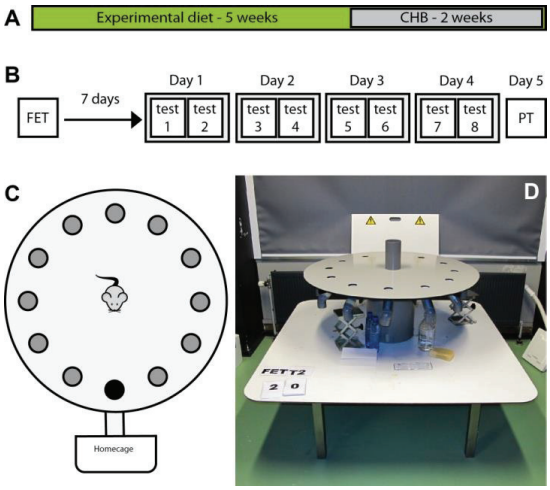

768 **Figure 5**

769

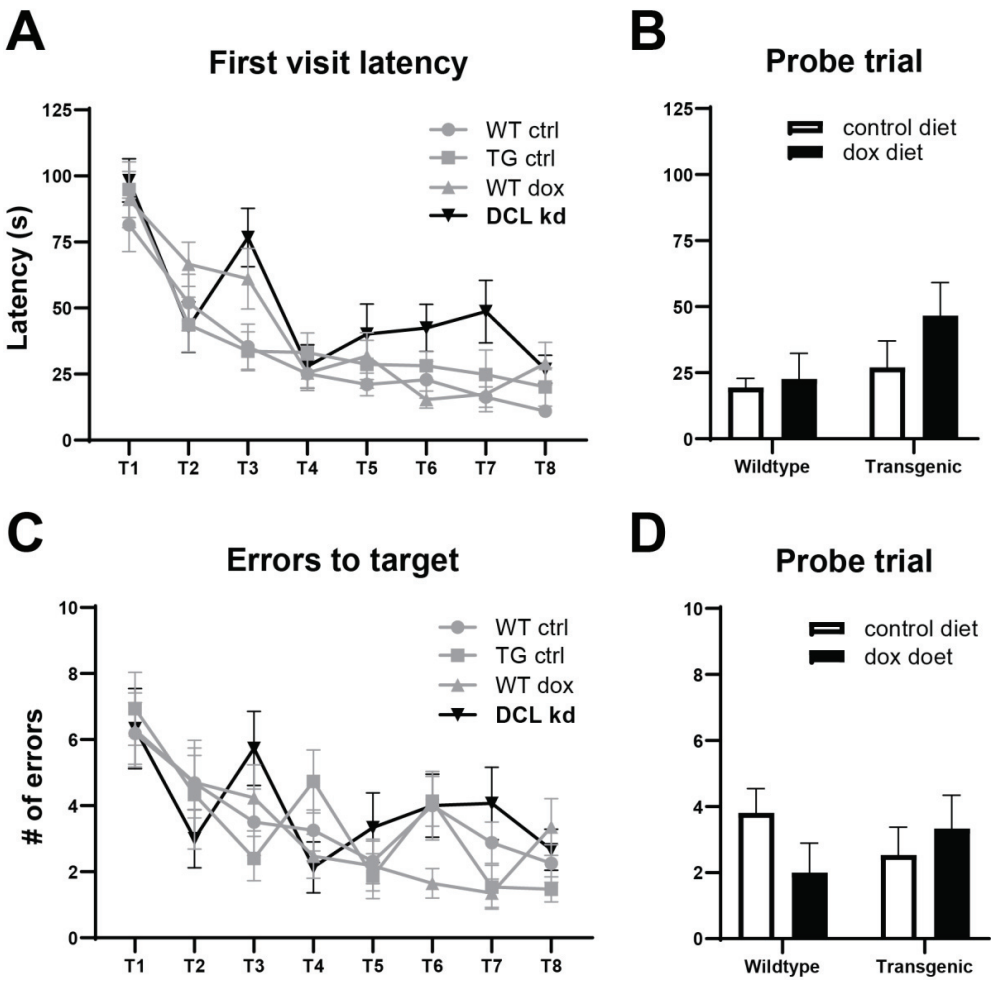

770

771

772 **Figure 6**

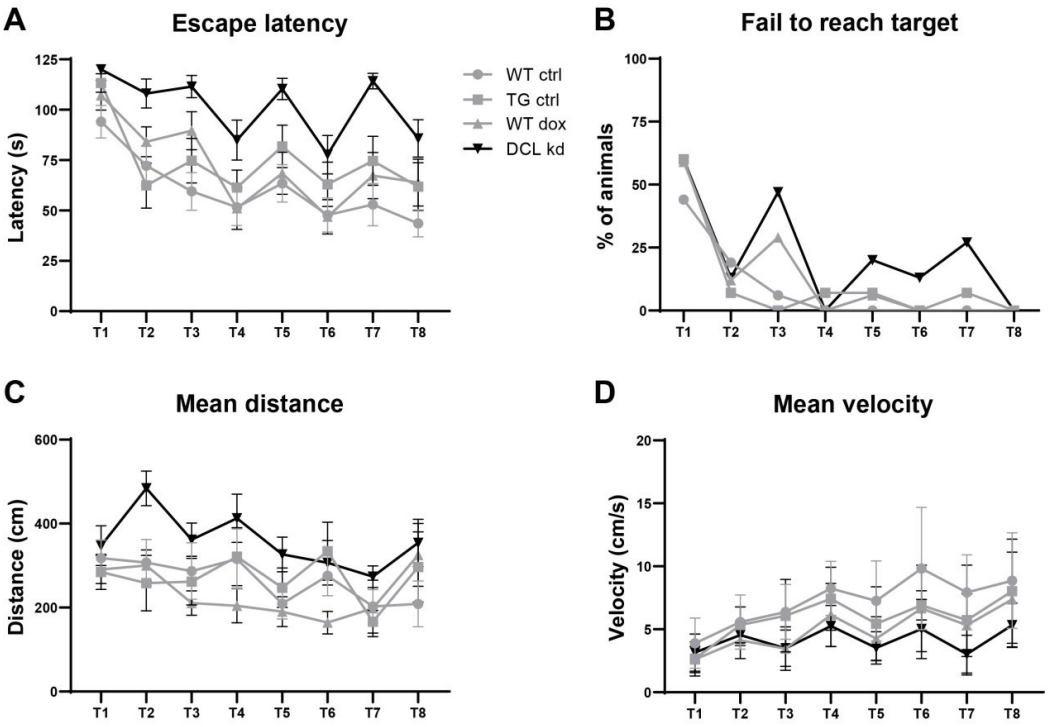

773

774